



IRAP Case Summaries

Case #1

Presenter: Aayushma Regmi, MBBS

Attending: Jodi J. Speiser, MD

Clinical History: A 43-year-old woman (G5P5) with past surgical history of total laparoscopic hysterectomy and bilateral salpingectomy for endometriosis and abnormal uterine bleeding presented with a palpable, pruritic, and minimally painful perineal lesion that occasionally bled. Physical examination revealed a 2.0 cm tender nodule at 7 o'clock in the right labia majora and multiple inclusion cysts in the left labia majora. A wide local excision of the lesion was performed. An H&E slide from the excision specimen of the right labia majora is provided for review. (Glass and scanned slides)

Final Diagnosis: **Deep Syringoma**

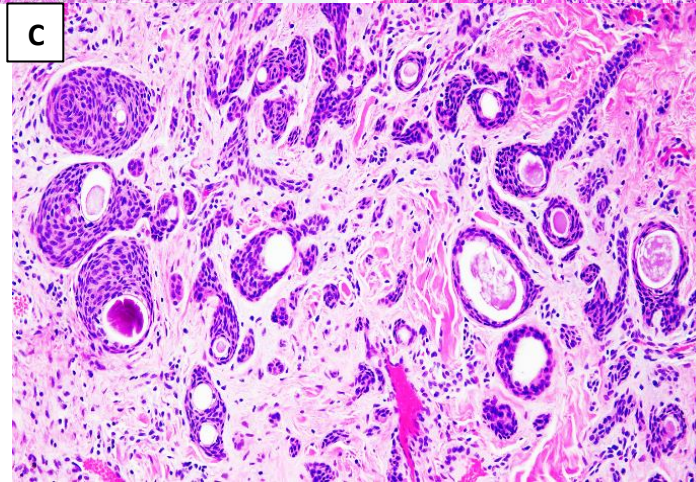
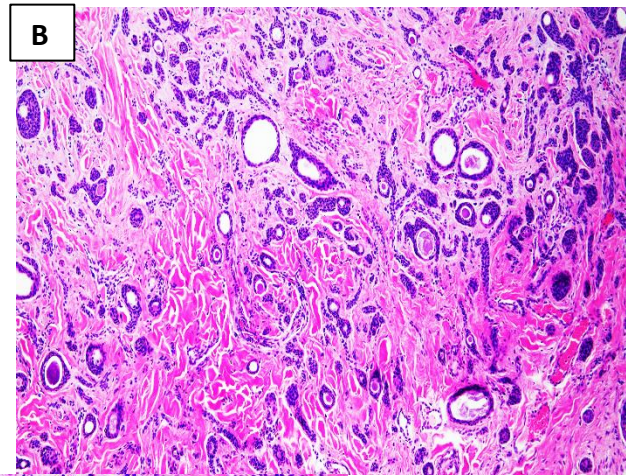
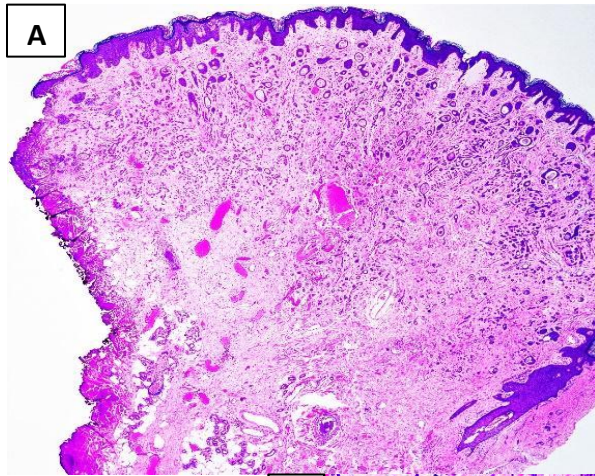
Differential Diagnosis:

- Metastatic adenocarcinoma
- Morpheaform basal cell carcinoma (MBCC)
- Desmoplastic trichoepithelioma (DT)
- Syringoid eccrine carcinoma (SEC)
- Deep syringoma
- Microcystic adnexal carcinoma (MAC)

Key Features:

Histopathology: H&E stained sections of the wide local excision showed an unremarkable epidermis with large, well-circumscribed dermal proliferation composed of small solid and ductal structures relatively evenly distributed in the sclerotic stroma (Figure A). There is also an extension of tumor to the deep reticular dermis. The epithelial elements consisted of monomorphous cuboidal cells with small nuclei having inconspicuous nucleoli and assumed round, oval, curvilinear or have other peculiar geometric shapes, including “comma-like” or “tadpole like” configurations (Figure B-C). The ductules are filled with eosinophilic amorphous luminal material. No follicular differentiation, cellular atypia or mitoses are identified. Also, in the sections examined, no perineural invasion was seen.





Positive IHC	Negative IHC
EMA	PR
CEA	S100
ER	





Discussion:

Syringoma is a benign adnexal tumor derived from intraepidermal luminal cells of eccrine sweat ducts. This tumor usually has a bilateral symmetrical distribution and presents as asymptomatic, multiple, small (1-5mm), smooth, skin-colored, dome-shaped papules. The periorbital area (the lower eyelid) is the most frequent anatomic location followed by scalp, forehead, neck, anterior chest, axillae, upper abdomen, and extremities. Vulvar region is considered as a rare anatomic location for syringoma. It was first reported by Carneiro in 1971 as usually affecting adolescent girls and middle-aged women at puberty or shortly thereafter. The cause of syringoma is unknown but studies have shown that hormonal influence and familial association are risk factors for syringoma. Although most syringomas occur sporadically, multiple syringomas may be inherited in autosomal dominant fashion; linked to Chromosome 16q22. Syringoma is also associated with multiple syndromes including Down, Ehlers-Danlos, Marfan, Nicoloau-Balus and Brook-Spiegler syndrome along with Hyperthyroidism. In addition, patients with vulvar syringomas usually have coexisting extragenital syringomas in the neck, eyelids, and periorbital area and so thorough examination of the body is essential.

Histopathologically, syringoma consists of a well circumscribed proliferation with 2 components including (1) epithelial cells forming ductules, nests, cysts and cords, and (2) stromal fibrosis/sclerosis. Epithelial cells are basaloid, cuboidal and double layered (in ductules) with an eosinophilic cuticle. Ducts are often described as comma or tadpole shaped or in a paisley pattern fibrotic stroma. No cytological atypia, mitosis, perineural invasion and follicular differentiation are identified. Syringoma usually occurs in the superficial dermis. Microscopically, syringoma must be differentiated from desmoplastic trichoepithelioma (DT), morpheaform/infiltrative basal cell carcinoma (MBCC), syringoid eccrine carcinoma (SEC) and microcystic adnexal carcinoma (MAC). We excluded DTE, MBCC, and SEC from our differential due to the lack of follicular differentiation, absence of cytological atypia, and lack of perineural invasion respectively.

Exclusion of MAC from our differential was challenging because of the patient's clinical presentation and morphological overlap with syringoma. Studies have shown that MAC and syringoma are misdiagnosed in 30% of the cases with superficial biopsies. MAC is a malignant adnexal tumor exhibiting dual ductal and follicular differentiation. They typically present as solitary, smooth, yellow or flesh-colored, slowly growing, indurated plaque or cystic nodule (average diameter of 2cm). It predominantly occurs in the head and neck region with a predilection for the centrafacial area including upper lips (74%), and nasolabial fold. Unlike syringomas, MACs usually infiltrate diffusely into dermis and subcutis and may extend into underlying muscle and bone. As atypia is minimal in both lesions, perineural invasion and follicular differentiation are the main distinguishing





features for MAC. A potential pitfall of misdiagnosis can be caused by superficial biopsies that reveal bland cytology and morphological overlap with syringoma, indicating a need for adequate tissue sampling for definitive diagnosis. Although our case had a similar clinical presentation and histology as MAC, the lack of follicular differentiation, atypia, mitoses and perineural invasion (on the sections examined) favored a syringoma with deep extension.

Distinction between MAC and syringoma is crucial to avoid undertreatment in MAC and overtreatment in syringoma. Treatment is seldom required in syringoma unless cosmetically indicated. Though the recurrence is frequent, various treatment options include oral/topical antibiotics, lasers, cryotherapy, electrosurgery, and excision. On the other hand, in MAC (malignant adnexal tumor), complete excision with clear margins is essential. In MAC the local recurrence is also high (up to 50%) with rare metastases.

This case presented many diagnostic challenges. The clinical presentation and anatomic location were unusual. Our case presented with an isolated painful solid lesion instead of multiple, painless, symmetrical lesions which are typical of vulvar syringomas. Histologically, the deep dermal extension of the tumor served as a potential pitfall for diagnosis, as syringomas are generally tumors of the superficial dermis. In the rare reported cases of vulvar syringoma (including one with deep dermal extension), the lesions were multiple. Thus, to our knowledge, our case is the first case of solitary vulvar syringoma with deep extension.

Though vulvar syringomas are rare, they should be considered in the differential diagnosis of any multicentric/solitary papular lesion of vulva. We encourage reporting of cases, particularly those with rare, atypical or unique presentations that can be helpful in diagnostically challenging situations to avoid potential diagnostic pitfalls.

Take Home Points:

1. Vulvar syringoma can be solitary and can present with involvement of deep reticular dermis
2. Vulvar syringoma should be considered as differential in case of any multicentric/solitary papular lesion of vulva
3. MAC and syringoma have morphological overlap and thus the diagnosis is challenging. Careful consideration should be taken before excluding anything from the differential to avoid misdiagnosis
4. When differentiating MAC versus a syringoma with deep dermal extension, the following clinical and pathologic factors should be examined to avoid misdiagnosis
 - A. Adequate tissue sampling





B. Clinical-pathological correlation

- I. Location
- II. Growth pattern/circumscription
- III. +/- Deep invasion
- IV. +/- Follicular differentiation
- V. +/- Perineural invasion

5. Reporting further cases of syringomas, particularly those with rare, atypical or unique presentations, will aid in further differentiating these similar entities and assuring that the patient gets the correct therapeutic intervention

References:

1. Kazakov DV, Bouda J Jr, Kacerovska D, Michal M. Vulvar syringomas with deep extension: a potential histopathologic mimic of microcystic adnexal carcinoma. *Int J Gynecol Pathol.* 2011 Jan;30(1):92-4. doi: 10.1097/PGP.0b013e3181ee5c9e. PMID: 21131826.
2. Suwattee P, McClelland MC, Huiras EE, Warshaw EM, Lee PK, Kaye VN, McCalmont TH, Niehans GA. Plaque-type syringoma: two cases misdiagnosed as microcystic adnexal carcinoma. *J Cutan Pathol.* 2008 Jun;35(6):570-4. doi: 10.1111/j.1600-0560.2007.00843.x. Epub 2007 Nov 12. PMID: 18005172.
3. Mitkov M, Balagula Y, Taube JM, Lockshin B. Plaque-like syringoma with involvement of deep reticular dermis. *J Am Acad Dermatol.* 2014 Nov;71(5):e206-7. doi: 10.1016/j.jaad.2014.04.005. PMID: 25437993.
4. Algeri P, Rodella R, Manfredini C, Algeri M. An Unusual Case of Genital Lesion: A Vulvar Syringoma. *J Family Reprod Health.* 2021 Mar;15(1):70-73. doi: 10.18502/jfrh.v15i1.6080. PMID: 34429739.
5. Miranda JJ, Shahabi S, Salih S, Bahtiyar OM. Vulvar syringoma, report of a case and review of the literature. *Yale J Biol Med.* Jul-Aug 2002;75(4):207-10. PMID: 12784970.
6. Blasdale C, McLelland J. Solitary giant vulval syringoma. *Br J Dermatol.* 1999 Aug;141(2):374-5. doi: 10.1046/j.1365-2133.1999.03012.x. PMID: 10468833.
7. Fallaha A, Thuile T, Tappeiner L, Pichler M, Deluca J, Perino F, Eisendle K. Misdiagnosed microcystic adnexal carcinoma on the lateral forehead and challenges in reconstruction of a large and bone-deep defect. *J Dtsch Dermatol Ges.* 2016 Jan;14(1):86-90. doi: 10.1111/ddg.12867. PMID: 26713651.
8. Garib G, Lullo JJ, Andea AA. Vulvar syringoma. *Cutis.* 2020 May;105(5):E7-E10. PMID: 32603397.
9. Henner MS, Shapiro PE, Ritter JH, Leffell DJ, Wick MR. Solitary syringoma. Report of five cases and clinicopathologic comparison with microcystic adnexal carcinoma of the skin. *Am J Dermatopathol.* 1995 Oct;17(5):465-70. PMID: 8599451.
10. Carneiro SJ, Gardner HL, Knox JM. Syringoma of the vulva. *Arch Dermatol.* 1971 May;103(5):494-6. PMID: 5580288.





Case #2

Presenter: Elnaz Panah, MD

Attending: Vijayalakshmi Ananthanarayanan, MBBS MD

Clinical History: A 78-year-old man with past medical history of coronary artery disease and IgG monoclonal gammopathy of undetermined significance (MGUS) presented to the emergency department with intermittent dizziness and progressive dyspnea. Bedside ultrasound showed pericardial effusion. An extensive workup led to a stress cardiac MRI that showed two separate masses, one in the right AV groove and another in the superior wall of the right atrium. Whole body PET/CT scan revealed increased uptake in the right AV groove, right atrium, and right adrenal gland. CT scan of the abdomen showed an extensive infiltrative process in the retroperitoneum that encased the aorta, renal hila, and bilateral adrenal glands. Adrenal gland biopsy was inconclusive. Fat pad biopsy showed kappa light chain deposition disease but no evidence of amyloid deposits. The patient underwent an endomyocardial biopsy of the right atrial mass, and a representative section of this specimen was submitted for review. (Scanned slide only)

Final Diagnosis: Erdheim-Chester Disease (ECD)

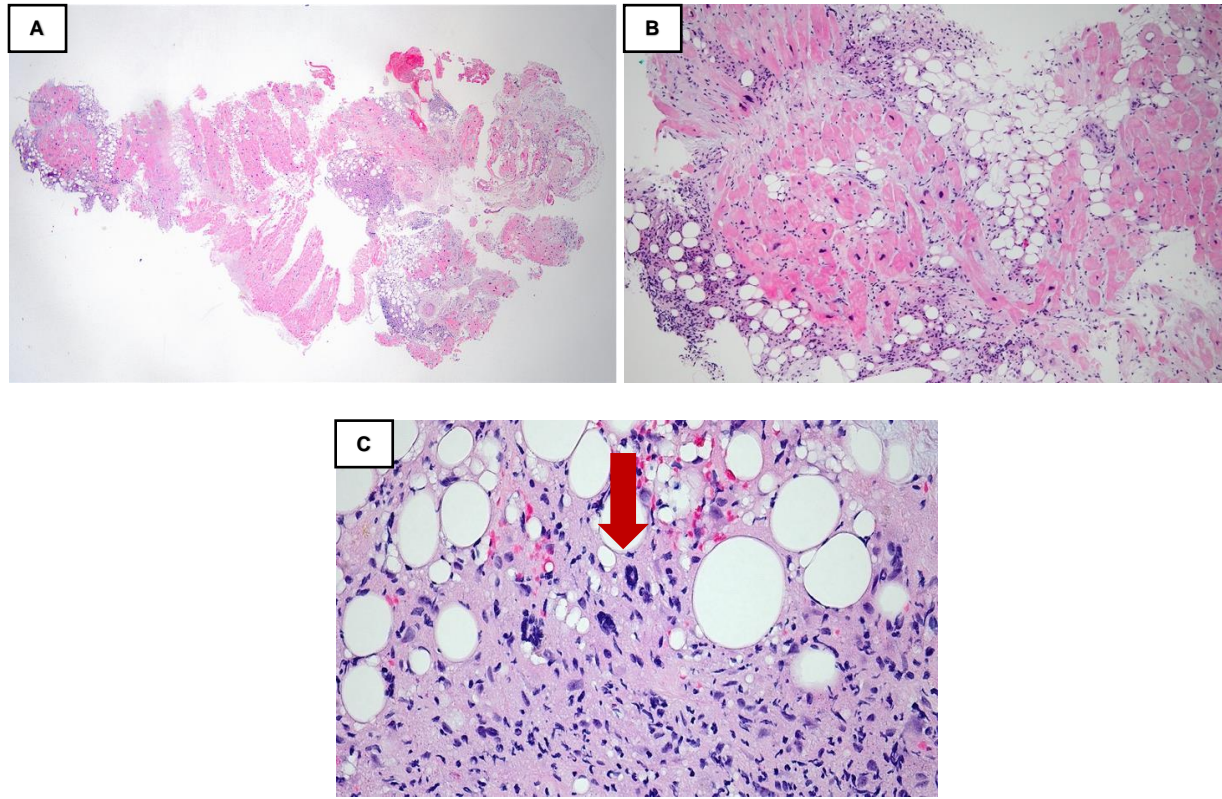
Differential Diagnosis:

- Fat Necrosis
- Lymphoma
- Juvenile Xanthogranuloma
- Rosai-Dorfman Disease (RDD)
- Langerhans Cell Histiocytosis (LCH)

Key Features:

Histopathology: H&E stained sections from the atrial biopsy show fragments of endomyocardium with increase in interstitial adipose tissue (Figure A). The myocytes show mild to moderate hypertrophy (Figure B). Infiltrating into the adipocytes are collections of histiocytes, lymphocytes, eosinophils. Multinucleated Touton-type giant cells are present (Figure C). Results of the immunophenotyping study by IHC are shown in the table below.





Positive IHC	Negative IHC	
CD68	AE1/AE3	CD20
Fascin	IgG4	CD30
CD163	SMA	Kappa
FXIIIa	CD34	Lambda
BRAFV600E	AFB	CD1a
	GMS	Langerin
	S100	

Discussion: ECD is a rare, non-Langerhans cell clonal histiocytic proliferation that was initially described by Jakob Erdheim and William Chester in 1930 (1). It typically affects adult males in the 5th and 7th decades of life (2). Clinical manifestations vary among different individuals and can be minimal to a life-threatening disease. Multiple organ systems can be affected including skin, bone, orbits, cardiovascular system, central nervous system, endocrine organ, respiratory system, retroperitoneal organs (3). It is considered a histiocytic neoplasm. Osseous involvement is most frequent and bilateral cortical sclerosis of the diaphysis is pathognomonic finding for ECD.

The diagnosis is often made on 99mTc Bone Scintigraphy or PET/CT scan and histology (4). Histologic features include non-Langerhans histiocytes with foamy or eosinophilic cytoplasm, xanthogranulomatosis, proliferating fibroblasts, lymphocytic aggregates, and Touton giant cells. On immunohistochemistry histiocytes are positive for Fascin, CD163, FXIIIa, BRAF V6000E and negative for Langerin, CD1a and S100





(3, 4). *BRAF V600E* mutation is the most common molecular mutation in ECD followed by *MAP2K1* alterations (1, 5).

While 42.5% of ECD patients are associated with clonal hematopoiesis and approximately 16% of patients develop a form of myeloid malignancy such as myeloproliferative neoplasms, chronic myelomonocytic leukemia, myelodysplastic syndrome, and acute myeloid leukemia (6), the association of ECD with lymphoproliferative disorder and monoclonal gammopathy is rather uncommon (7).

Take Home Points:

ECD is a rare histiocytic neoplasm with unknown etiology. It is a multisystem disorder, most commonly affecting bone. Histologic features include Xanthomatous histiocytes and Touton giant cells. Histiocytes are positive for CD68, CD163, FXIIIa, *BRAF V600E* and negative for Langerin, CD1a and S100. *BRAF V600E* mutation is the most common molecular mutation following by *MAP2K1*. ECD is associated with a high frequency of clonal hematopoiesis and myeloid malignancies.

References:

1. Ozkaya N, Rosenblum MK, Durham BH, Pichardo JD, Abdel-Wahab O, Hameed MR, et al. The histopathology of Erdheim-Chester disease: a comprehensive review of a molecularly characterized cohort. *Mod Pathol*. 2018;31(4):581-97.
2. Mazor RD, Manevich-Mazor M, Shoenfeld Y. Erdheim-Chester Disease: a comprehensive review of the literature. *Orphanet J Rare Dis*. 2013;8:137.
3. Goyal G, Young JR, Koster MJ, Tobin WO, Vassallo R, Ryu JH, et al. The Mayo Clinic Histiocytosis Working Group Consensus Statement for the Diagnosis and Evaluation of Adult Patients With Histiocytic Neoplasms: Erdheim-Chester Disease, Langerhans Cell Histiocytosis, and Rosai-Dorfman Disease. *Mayo Clin Proc*. 2019;94(10):2054-71.
4. Roh J, Muelleman T, Tawfik O, Thomas SM. Perineural growth in head and neck squamous cell carcinoma: a review. *Oral Oncol*. 2015;51(1):16-23.
5. Diamond EL, Dagna L, Hyman DM, Cavalli G, Janku F, Estrada-Veras J, et al. Consensus guidelines for the diagnosis and clinical management of Erdheim-Chester disease. *Blood*. 2014;124(4):483-92.
6. Cohen Aubart F, Roos-Weil D, Armand M, Marceau-Renaut A, Emile JF, Duployez N, et al. High frequency of clonal hematopoiesis in Erdheim-Chester disease. *Blood*. 2021;137(4):485-92.
7. Pavlidakey PG, Mohanty A, Kohler LJ, Meyerson HJ. Erdheim-Chester disease associated with marginal zone lymphoma and monoclonal proteinemia. *Case Rep Hematol*. 2011;2011:941637.





Case #3

Presenter: Sandra Haddad, MD (PGY-II)

Attending(s): Güliz A. Barkan, MD; Dr. Mohammed K. Atieh, DO, MS; Dr. Swati Mehrotra, MD; Vijayalakshmi Ananthanarayanan, MD; Khin Su Mon, MD; Ayse Irem Kilic, MD

Clinical History: A 78-year-old man presented to the ER with worsening shortness of breath. He has a past medical history of chronic respiratory failure, hypertension, anemia, and deep vein thrombosis. He had no fever, cough, chest pain, or palpitations. He is status post left thyroidectomy for multinodular goiter. Physical exam was significant for diminished breath sounds in the base of the left lung, as well as bilateral lower extremity pitting edema (+1). Imaging studies showed left-sided pleural effusion, numerous lung nodules, and mediastinal lymphadenopathy. Thoracentesis was performed; a ThinPrep and a cell block section prepared from the left pleural fluid are provided for review.

Final Diagnosis: Metastatic salivary duct carcinoma

Differential Diagnosis:

- Mesothelial cells with reactive atypia
- Metastatic adenocarcinoma:
 - Lung
 - Breast
 - Colorectal
 - Gastric
 - Prostate
 - Pancreatobiliary
- Malignant mesothelioma
- Epithelioid angiosarcoma

Key Features:

Cytology: ThinPrep slides showed a moderately cellular specimen. There were occasional lymphocytes and numerous moderately variable sized, round to polygonal tumor cells with abundant finely granular to vacuolated cytoplasm, and nuclei with prominent nucleoli (Figure-1). The tumor cells were present as isolated cells and 3-dimensional groups (Figure-2). Cell block revealed clusters and isolated cells clustered in the lacunae and forming glandular pattern with vaguely cribriforming in some areas (Figure-3).



Figure - 1

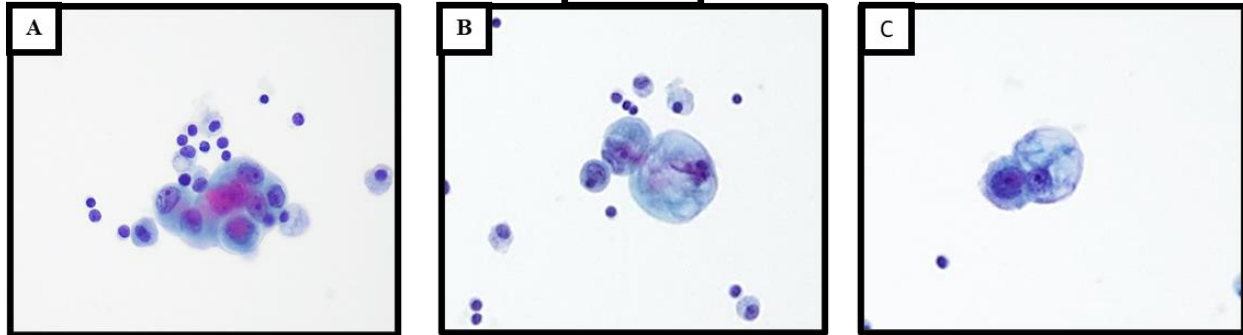


Figure - 2

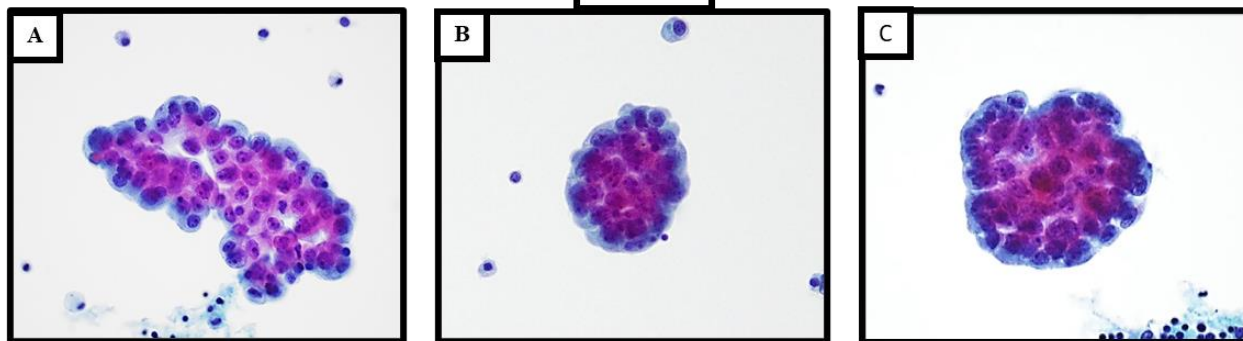
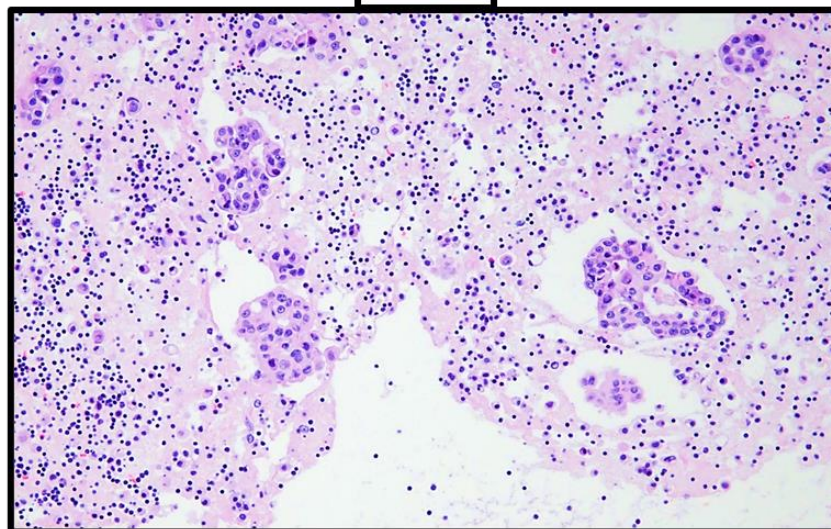


Figure - 3





Positive IHC for tumor cells	Negative IHC for tumor cells
CK7	CK20
MOC-31	D2-40
BerEP4	TTF-1
GATA-3	Napsin-A
AR	P40
HER-2	CDX2
	NKX3.1
	Calretinin

Discussion:

Salivary duct carcinoma (SDC) is a relatively rare tumor, first described by Kleinsasser et al in 1968, accounting for approximately 9-10% of all salivary gland malignancies. In 40% of cases arise as carcinoma ex pleomorphic adenoma. Most common in elderly population (peak: 6th-7th decades). There is a male predominance of 2-4:1. Most common site for primary SDC is the parotid gland in 70-95% of cases. Less commonly in the submandibular gland, rarely in the sublingual gland, and uncommon in the maxillary sinus and larynx. Tumor is highly aggressive with poor overall prognosis and there is a high rate of lymph nodes or distant metastasis at initial presentation (60-70%). The lung is a frequent site of metastatic disease, although lesions in liver, bone, thyroid, skin, vagina, brain, and eye have also been described. Very rare cases of metastatic salivary duct carcinoma to the pleural fluid have been reported.

Histomorphologically, it is a high-grade apocrine adenocarcinoma resembling mammary ductal carcinoma with a mixed pattern consisting of nests, cribriform, micropapillary, sarcomatoid, mucin-rich, and osteoclast-type giant cell patterns. It is characterized by comedonecrosis and Roman-bridge appearance. Peri-intra neural invasion is common. Mutations or amplification of *PIK3CA*, and loss of *PTEN* are reported. HER2 gene amplification detected by FISH in 10-30% of cases. *EGFR* mutations ~10% (there is no positive correlation between *EGFR* and *ERBB2* alterations-independent roles), and *HRAS* hotspot mutations ~ 30%. In case of carcinoma-ex-pleomorphic adenoma, it may overexpress translocation associated proteins PLAG1 or HMGA2.

The effusion cytology appearance of salivary duct carcinoma includes the presence of cohesive 3D clusters and flat sheets with cribriform/papillary architecture and dirty necrotic background. Neoplastic cells are round to polygonal with rich eosinophilic finely granular to vacuolated cytoplasm and large nuclei containing prominent nucleoli. Also, isolated, individual atypical epithelial cells scattered at periphery of clusters. Hence these features of high-grade adenocarcinoma in an effusion, can be very challenging to differentiate from other metastatic adenocarcinomas, malignant mesothelioma, or even mesothelial cells with reactive atypia, it is important to perform





immunohistochemical stains on the cell block. Neoplastic cells will show diffuse strong nuclear staining for Androgen receptor (AR) in 95% of cases. It can be also positive for GCDPF-15 (~ 80%), CK7, GATA-3, EMA, AE1/AE3, PSA (~57%), HER2/neu (+2) (~35%) and mucicarmine in mucin rich variant. Expression of AR, GCDPF-15, and HER2 can confirm the diagnosis of a salivary duct carcinoma. Our case illustrates an unusual spread of SDC into the pleural fluid and highlights the challenges in rendering a diagnosis of metastatic SDC on a cytology specimen alone.

Distant metastases are the primary cause of treatment failure in patients with salivary duct carcinoma. There is no consensus on the standard treatment. Trastuzumab (Herceptin) may be used as adjuvant therapy in patients with HER2/neu tumors that are FISH positive, however, it is experimental, and the efficacy of therapy is still unclear.

Take Home Points:

- Development of pleural metastasis of salivary gland carcinoma is extremely rare and highly aggressive
 - Diagnosis is very challenging on a cytology specimen (morphology alone)
 - If it is not impossible, it is very hard to differentiate from metastatic adenocarcinomas as they mimic each other
 - Clinical history is very critical
- In the effusion cytology having cohesive 3D clusters, flat sheets with cribriform/papillary architecture and a dirty necrotic background in an older individual with a salivary gland mass, can be a helpful clue for the diagnosis of metastatic SDC
- Expression of AR, GCDPF-15, and HER2 confirms the diagnosis
- Role of HER2 targeted therapy in this setting is still unclear
 - Experimental therapy of Herceptin may be used as adjuvant therapy in patients with HER2/neu tumors that are FISH positive

References:

1. Han MW et al: Prognostic factors and outcome analysis of salivary duct carcinoma. *Auris Nasus Larynx*. 42(6):472-7, 2015
2. Mimica X, McGill M, Hay A, et al. Distant metastasis of salivary gland cancer: Incidence, management, and outcomes. *Cancer* 2020
3. Bahrami A et al: An analysis of PLAG1 and HMGA2 rearrangements in salivary duct carcinoma and examination of the role of precursor lesions. *Histopathology*. 63(2):250-62, 2013
4. Salivary Duct Carcinoma: Updates in Histology, Cytology, Molecular Biology, and Treatment. May 2020, PMID: 32421944





5. Metastatic salivary duct carcinoma in cardiac and pleural effusions: A case report with immunocytochemical analysis for androgen receptor and HER2. 2018. PMID: 30655980
6. Salivary Duct Carcinoma: An Update on Morphologic Mimics and Diagnostic Use of Androgen Receptor Immunohistochemistry
7. An Aggressive Salivary Gland Carcinoma with Morphologic Variants, Newly Identified Molecular Characteristics, and Emerging Treatment Modalities. January 2021
8. Pleural fluid metastases of salivary duct carcinoma: A case report and review of the literature. 2014. PMID:24738005
9. Williams MD et al: Genetic and expression analysis of HER-2 and EGFR genes in salivary duct carcinoma: empirical and therapeutic significance. Clin Cancer Res. 16(8):2266-74, 2010
10. Schwartz LE et al: GATA3 immunohistochemical expression in salivary gland neoplasms. Head Neck Pathol.7(4):311-5, 2013
11. Nakashima T et al: Is there a role of adjuvant treatment for salivary duct carcinoma? J Laryngol Otol. 129 Suppl 2: S98-101, 2015
12. Salivary duct carcinoma: Clinicopathologic features, morphologic spectrum, and somatic mutations. PMID: 26699379, 2016
13. Frequent PTEN loss and differential HER2/PI3K signaling pathway alterations in salivary duct carcinoma: Implications for targeted therapy. PMID: 30289966
14. The International System for Serous Fluid Cytopathology, https://doi.org/10.1007/978-3-030-53908-5_1
15. Milan System for Reporting Salivary Gland Cytopathology
16. <https://www.pathologyoutlines.com/topic/salivaryglandssalivaryductcarcinoma.html>





Case #4

Presenter: Constantine E. Kanakis, MD MSc

Attending: Kamran Mirza, MD PhD and Milind Velankar, MD

Clinical History: A 74-year-old male with a past medical history of hypertension, hyperlipidemia, glaucoma, benign prostatic hyperplasia, and well-controlled ulcerative colitis presented with persistent bilateral cervical lymphadenopathy after a recent viral upper respiratory infection. He denied any associated fevers, chills or night sweats but endorsed slow intentional weight loss over the preceding few months. Review of symptoms was positive for hearing loss, cough, and joint pain. He leads an active lifestyle, has a vegetarian diet, and retired from work as a veterinarian. No toxic habits or relevant family history was reported. Computed tomography (CT) of the neck visualized the lymphadenopathy and hypoechoic region near the left submandibular gland. A fine needle aspiration (FNA) of the left submandibular gland was non-diagnostic. A subsequent excisional biopsy was performed.

(Digitally scanned slides provided)

Final Diagnosis: Angioimmunoblastic T-cell Lymphoma (Pattern 1) with an Atypical Monoclonal Ig-Kappa B-cell Clone

Differential Diagnosis:

- | | |
|---|---------|
| • Nodular lymphocyte-predominant Hodgkin lymphoma | NLPHL |
| • T-cell/histiocyte rich large B-cell lymphoma | THRLBCL |
| • Classic Hodgkin lymphoma | CHL |
| • Anaplastic large cell lymphoma | ALCL |
| • Follicular T-helper cell lymphoma | FTHL |
| • Nodal Peripheral T-cell Lymphoma with TFH phenotype | F-PTCL |
| • Angioimmunoblastic T-cell Lymphoma | AITL |

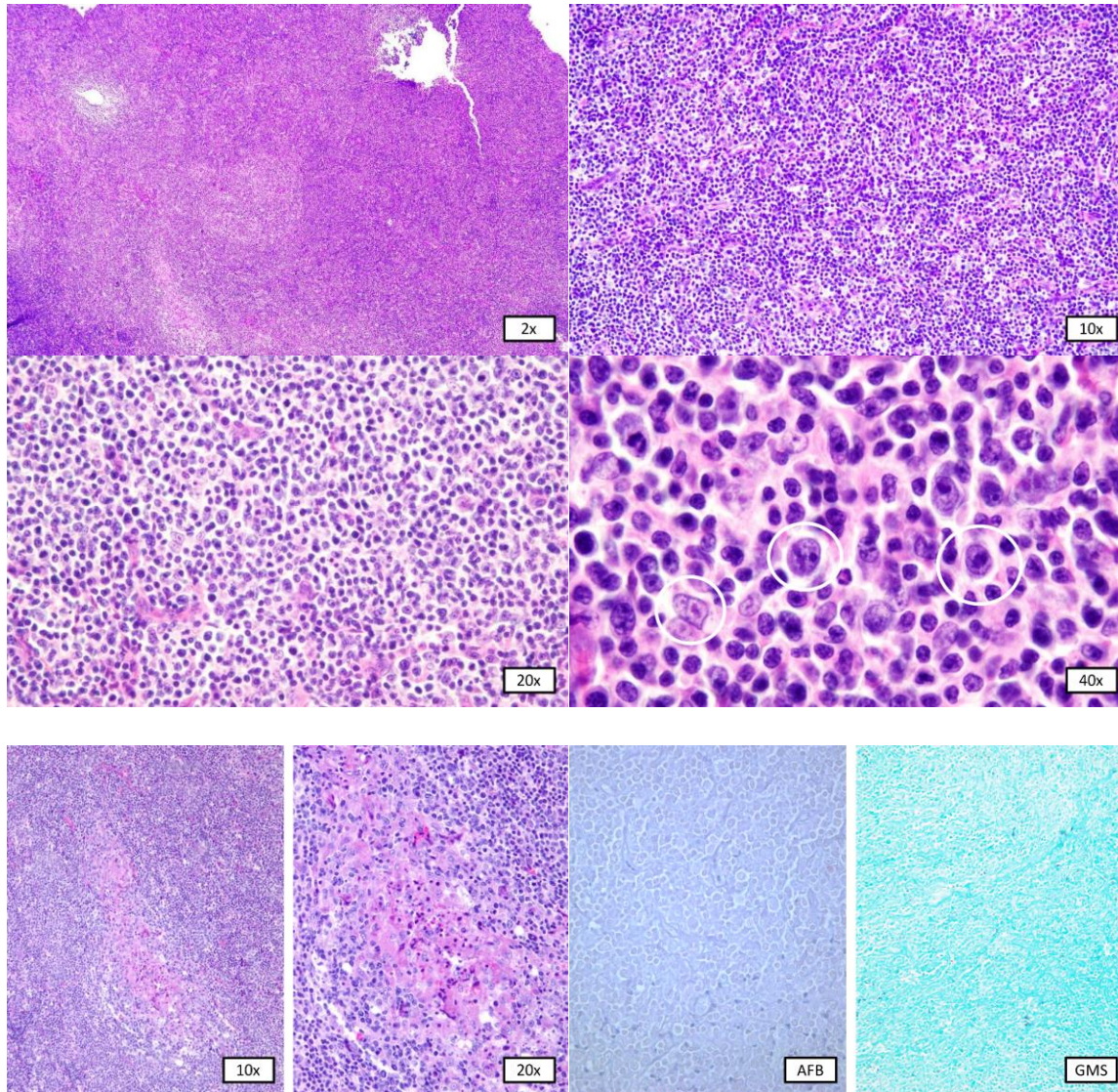
Key Features:

Histopathology: Histologic examination of the biopsied lymph node fragments demonstrated somewhat preserved follicular architecture with expansion in the paracortical region. There is a predominance of small, round mature lymphocytes



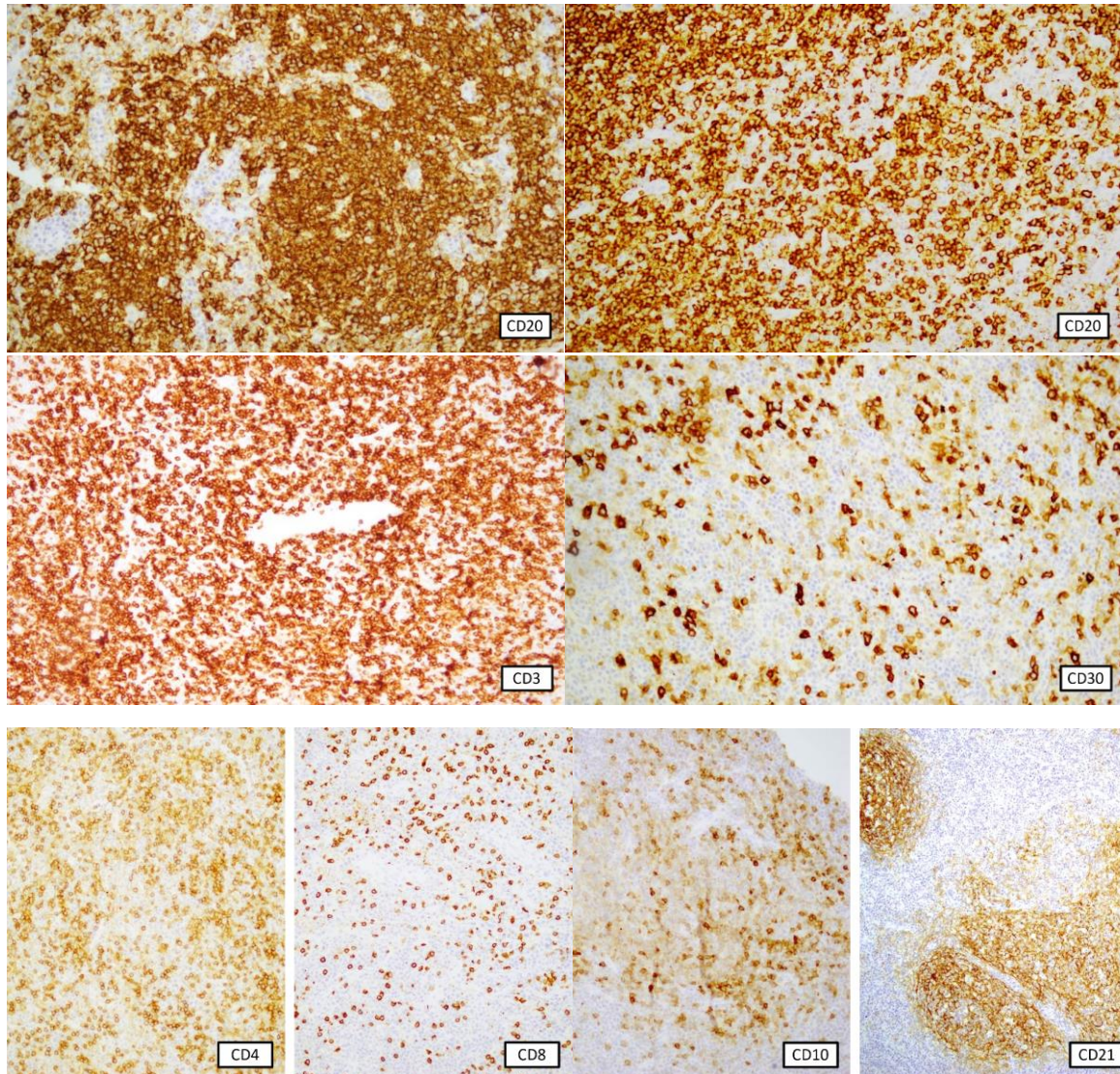


punctuated by occasional atypical large cells and densely surrounded increased high endothelial venules. Higher power reveals the larger, atypical cells surround germinal centers and there is a dense expansion of the paracortical zone. There are few germinal centers which demonstrate necrosis with central debris and pseudo-granulomatous inflammation. Cytologic atypia is mostly seen in the scattered large cells. Stains for infectious etiologies (AFB/GMS) were negative.



Immunohistochemical staining patterns revealed a strong follicular CD20 with expansion into the paracortex, diffusely positive CD3, CD4, and CD8 with an increased CD4:CD8 ratio. CD30 highlighted the large, atypical cells. CD10 highlighted preserved germinal center architecture with CD21 demonstrating expanded follicular dendritic cell meshwork beyond the germinal centers. In-situ hybridization for EBV highlighted focal, scattered cells.





Discussion

This patient's clinical presentation of lymphadenopathy without major B-cell symptoms promptly incited a lymphoma workup which included concurrent laboratory studies and ancillary tests. Their laboratory results were overall unremarkable with the exception of slightly increased IgG and free light chain (kappa) concentrations. Flow cytometry did not show any increase in blasts or expanded monoclonal populations but did show slight predominance of CD19+ kappa+ B-cells. T-cell and B-cell gene rearrangement was done and showed T-cell rearrangements in both the receptor gamma and beta genes, as well as in the kappa light immunoglobulin chain in the B-cells. Histologically, the important hallmarks to recognize are the somewhat preserved follicular architecture with expanded paracortical/follicular dendritic cell meshwork involving scattered large, atypical cells and increased high endothelial venules. While this initially may lead to a



differential that is led by angioimmunoblastic T-cell lymphoma (ATIL), the question of the expanding B-cell clone is unanswered. A differential diagnosis was made based on findings of atypical large cells in a background of expanded small cells, to include possible entities of both B-cell and T-cell lineage.

The patterns of preserved follicular architecture with large, atypical cells and high endothelial venules can be difficult to distinguish from atypical cells expanding from the marginal or mantle zones, paracortex, or medullary regions. Therefore, pattern recognition, gene rearrangement, and immunohistochemistry all contribute to a confirmatory assessment of this diagnosis of ATIL pattern 1.

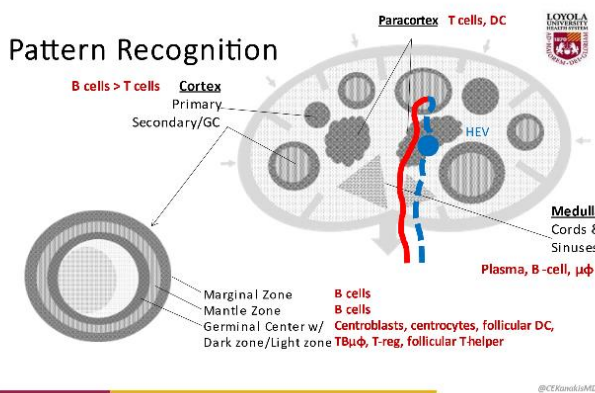


Figure 1. Regarding entities in hematopathology, particularly nodal subtypes, the differential in our case was predicated on lymphoid architectural patterns. Recognizing what cells predominate in various regions of lymph nodes, is critical to building and excluding from a broad differential. While seeing expected increases in B-cells in proliferative germinal centers is expected from various causes, the expansion of these cells into the paracortex is irregular and may indicate clonal expansion or other malignant processes.

ATIL occurs in three distinct architectural patterns, namely 1, 2, and 3. Increasing in number loosely translates to an increase in severity, as nodal architecture, follicular activity, FDC meshwork, and atypia trend upwards toward pattern 3. Our case demonstrated largely preserved follicular and nodal architecture (in a fragmented biopsy), hyperplastic B-cell follicles with attenuated mantle cuffs, expansion of FDCs around the germinal centers with atypical T-cells in the perifollicular space in a background of polymorphic infiltrate and high endothelial venules.

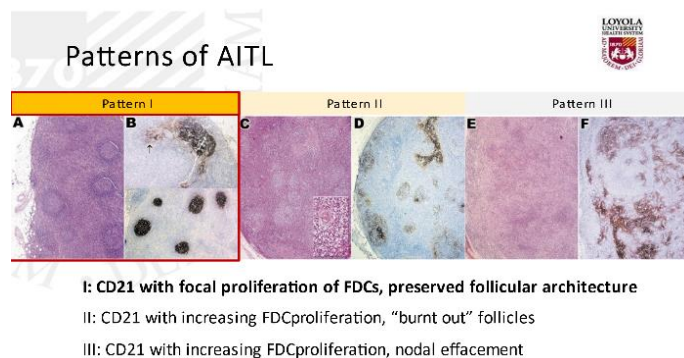


Figure 2. Staining for CD21 can effectively demonstrate the progressive effacement of nodal architecture from patterns 1 to 3. With pattern 1 demonstrating focal FDC proliferation and overall preserved follicular structure, pattern 3 culminates in the completed “burn out” of follicles and even more meshwork proliferation. The architecture becomes completely effaced by the perifollicular expansion.

Allyette, Armand, Akbari, Raju & Tsoi, T. A. (2018). The 2018 WHO Classification of Lymphoid Neoplasms. *Journal of Cellular Biochemistry*, 123(1), 1-10. doi:10.1002/jcb.23827

Patil, M., Ghosal, S., Ghosh, B., et al. (2018). Subclassification of Angioimmunoblastic T-cell lymphoma: a clinical and immunohistochemical study. *Journal of Cellular Biochemistry*, 123(1), 1-10. doi:10.1002/jcb.23827



Based on these patterns and supporting evidence in diagnosing AITL, the consideration of the expanded B-cell clone becomes important—particularly to determine whether or not the B-cells are, in fact, related to the primary diagnosis or represent a potential, concurrent malignancy. Composite B and T-cell lymphomas can be difficult to assess but an understanding of pathophysiologic processes in our diagnosis, in part, answers this clinical question.

In AITLs there are several T-cell mutations that occur in the genomic development of malignant T-cell proliferation. To note, two specific mutations in methylating regions can affect T-cell receptor activity downstream: *TET2* and/or *DNMT3A*. The mutations can affect the T-cell-B-cell interactions enabled by T-cell receptors with primed, mutated T-follicular helper cells as they possibly acquire further mutations in *RHOH* and *IDH2*, which further affect T-cell signaling. As these T-cells mutate, and proliferate, their malignant clone continues to activate B-cells within the lymph node. Activated B-cells can also acquire the *TET2* and/or *DNMT3A* mutations along with downstream effects of possible EBV positivity and/or *NOTCH1*, increasing these signaling pathways further in what is, essentially, a multi-hit cycle of acquired upregulating mutations. Increased activity of T-cells with affected gene-rearranged receptors, can create a subpopulation of B-cells clones in this setting.

Finally, the occasional necrotic germinal centers were not wholly explained. Originally designated as “immunodysplastic disease,” AITL may histologically feature various polymorphous infiltrates to include possible granulomatous inflammation and even vasculitis. This has been reported in literature sparsely.

Take-home Points

- Recognizing nodal architectural patterns and the translated implications of cell origins led to the diagnosis of an atypical T-cell infiltrate with features consistent with angioimmunoblastic T-cell lymphoma (AITL) pattern 1
- IGK B-cell population is uncertain significance, but can be seen in AITL, necrotic germinal centers in unclear/not always in AITL
- Even in a lineage-specific lymphoid neoplasm, it is important to recognize and address other clonal populations of B or T cells
- Entities like AITL may feature additional clonal cell expansions of B-cells and may cause phenotypic confusion with reactive, infectious, or neoplastic processes – it is important to carefully distinguish reactive, pathophysiologic, or malignant processes in potential composite lymphoma diagnoses





References

1. Matthew A. Lunning, Julie M. Vose; Angioimmunoblastic T-cell lymphoma: the many-faced lymphoma. *Blood* 2017; 129 (9): 1095–1102. doi: <https://doi.org/10.1182/blood-2016-09-692541>
2. Chiba, S., Sakata-Yanagimoto, M. Advances in understanding of angioimmunoblastic T-cell lymphoma. *Leukemia* **34**, 2592–2606 (2020). <https://doi.org/10.1038/s41375-020-0990-y>
3. <https://www.immunology.org/public-information/bitesized-immunology/cells/t-follicular-helper-cells>
4. Ayoma Attygalle, Rajai Al-Jehani, Tim C. Diss, Phillipa Munson, Hongxiang Liu, Ming-Qing Du, Peter G. Isaacson, Ahmet Dogan; Neoplastic T cells in angioimmunoblastic T-cell lymphoma express CD10. *Blood* 2002; 99 (2): 627–633. doi: <https://doi.org/10.1182/blood.V99.2.627>
5. Yi Xie, MD, PhD, Elaine S Jaffe, MD, How I Diagnose Angioimmunoblastic T-Cell Lymphoma, *American Journal of Clinical Pathology*, Volume 156, Issue 1, July 2021, Pages 1–14, <https://doi.org/10.1093/ajcp/aqab090>
6. Bal M, Gujral S, Gandhi J, Shet T, Epari S, Subramanian P G. Angioimmunoblastic T-Cell lymphoma: A critical analysis of clinical, morphologic and immunophenotypic features. *Indian J Pathol Microbiol* 2010;53:640-5
7. Bhatlapenumarthy, V., Patwari, A., & Pascual, S. K. (2020). Diagnostic Dilemma: An Unusual Case of Angioimmunoblastic T-Cell Lymphoma Manifesting as Bone Marrow Non Caseating Granuloma. *Journal of hematology*, 9(1-2), 37–40. <https://doi.org/10.14740/jh607>
8. Swarup, Sriman & Kopel, Jonathan & Kyaw, Zin & Thein, Kyaw & Tarafdar, Kaiser & Swarup, Khatrina & Thirumala, Seshadri & Quick, Donald. (2021). Sequential Complications of Hypercalcemia, Necrotizing Granulomatous Vasculitis, and Aplastic Anemia Occurring in One Patient with Angioimmunoblastic T-cell Lymphoma. *The American Journal of the Medical Sciences*. 361. 375–382.





Case #5

Presenter: Levent Trabzonlu, MD

Attending: Maria M. Picken, MD, PhD

Clinical History: A 75-year-old man with past medical history of hypertension presents to an outside clinic with left lower abdominal quadrant pain. On imaging, a right renal lesion is incidentally found and the patient is directed to our institution. His renal function is normal. In-house MRI shows an exophytic lesion arising from the lower pole of the right kidney measuring 3.2 cm in greatest dimension. No invasion to the pelvicalyceal system or renal vein is identified. A partial nephrectomy is performed. A representative section is scanned and provided for review.

Final Diagnosis: Papillary renal cell carcinoma with reverse polarity

Differential Diagnosis

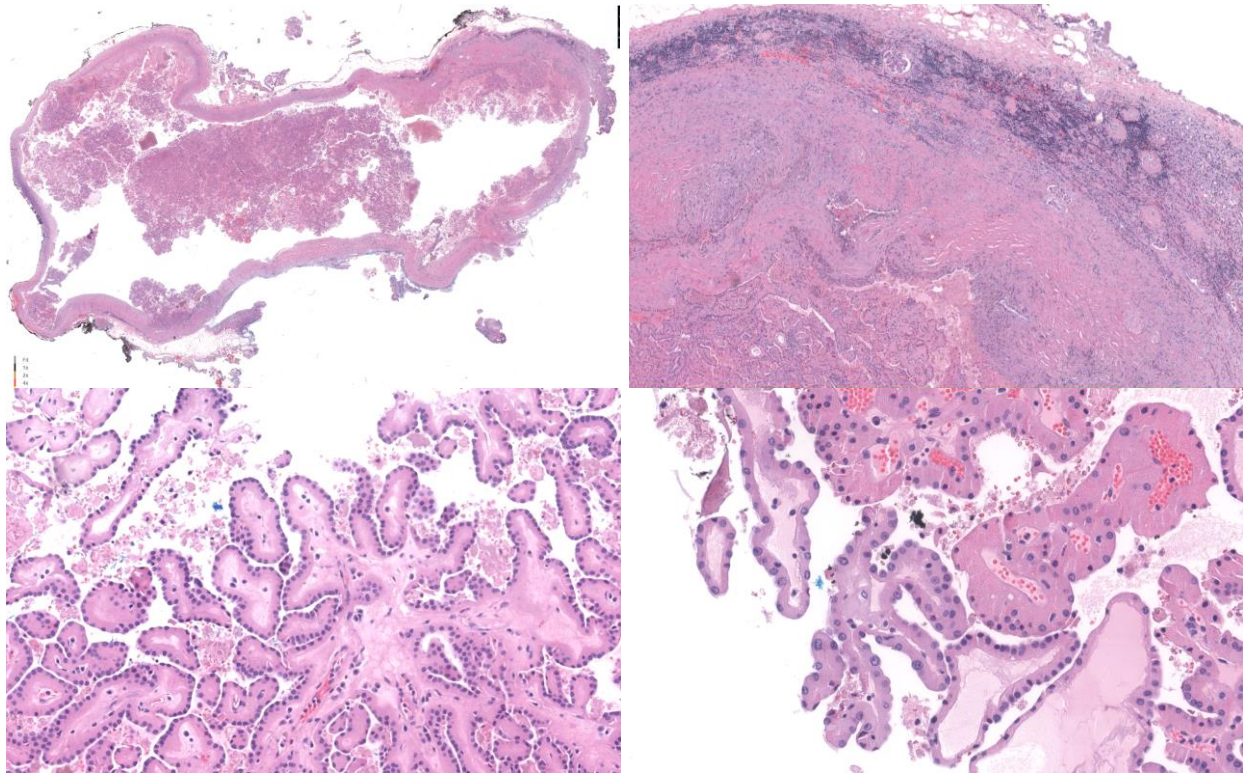
- Papillary renal cell carcinoma, type-1
- Papillary renal cell carcinoma, type-2
- Oncocytic papillary renal cell carcinoma
- Eosinophilic solid and cystic renal cell carcinoma
- Clear cell papillary renal cell carcinoma
- Xp11 translocation renal cell carcinoma
- Papillary urothelial carcinoma
- Metastasis of tall cell carcinoma with reverse polarity of the breast
- Metastasis of papillary thyroid carcinoma, tall cell variant

Key Features:

Histopathology: The section shows a well-circumscribed, largely cystic lesion with a pseudocapsule. Adjacent kidney shows secondary atrophic changes due to compression. The more solid areas of the lesion show mostly papillary structures with true fibrovascular cores. The lining epithelial cells are mostly uniform, and bland-appearing. The cells have large eosinophilic cytoplasm and apically arranged nuclei. Other areas with oncocytic cells and hobnail cells are also noted.

Positive IHC for tumor cells	Negative IHC for tumor cells
GATA3	Vimentin
CK7	Keratin 34BE12
EMA	CD15
Racemase	





Discussion:

Papillary renal cell carcinoma with reverse polarity is an emerging entity that has been referred to in the literature as "oncocytic low-grade papillary RCC" and "type 4 papillary RCC". It has distinct morphology, IHC profile, and recurrent molecular alterations. They are usually small and cystic lesions with no reported progression in the literature to date. The classic morphology is defined as oncocytic cells arranged in a tubulopapillary architecture with low-grade nuclei (WHO/ISUP Grade 1-2) that are apically located in the cytoplasm. These tumors are uniformly positive for GATA3 and CK7 with variable expression for vimentin and Racemase. Most cases harbor *KRAS* mutations (80-90%).

GATA3 expression and *KRAS* mutations suggest this may be a unique tumor. However, the presence of papillary architecture and the molecular alterations that are seen in papillary RCC such as trisomy 7 and 17, and loss of chromosome Y suggest that this is a subtype of papillary RCC.

GATA3 expression has been shown in a variety of renal neoplasms such as clear cell papillary RCC, oncocytoma, and chromophobe RCC. It is a transcription factor that plays important role in the nephron development. Its expression is high in the distal and collecting ducts and low in the proximal tubules. This profile is in line with GATA 3 expression in benign and malignant renal lesions. For example, in glomerulocystic renal disease that originates from Bowman's capsule and proximal tubules, the cyst lining is negative for GATA3. On the other hand, in polycystic kidney disease that originates from the distal tubules, the cyst lining is positive for GATA3. Similarly, clear cell RCC and papillary RCC that originate from proximal tubules are negative for GATA3. Oncocytoma and





chromophobe RCC that originate from the junction of loop of Henle are positive for GATA3 in 50% of tumors. Clear cell papillary RCC is considered to originate from the distal tubules and is positive for GATA3. Therefore, it is reasonable to suggest that papillary RCC with reverse polarity may originate from the distal portion of nephron. However, ultrastructural and molecular analyses are needed to further support this proposal.

Differential diagnosis includes other papillary tumors of the renal parenchyma. Although the classification of papillary RCCs into types 1 and 2 is still in place, new publications recommend not to use it because of the subjectivity, mixed features in a large proportion of cases and lack of proven clinical value of this classification. There are multiple new variants included in the spectrum of papillary RCC with specific morphology, immunoprofile, and predicted clinical behavior. Papillary RCC with reverse polarity is a distinct entity with its classic morphology and unique GATA3 expression and *KRAS* mutations.

Take Home Points:

- Papillary RCC with reverse polarity is an emerging entity that has unique morphologic, immunophenotypic, and molecular features.
- These are indolent tumors with no reported progression.
- Papillary renal tumor with abundant eosinophilic cytoplasm and apically located low-grade nuclei is the defining morphology.
- Combination of GATA3 expression and *KRAS* mutations is a distinguishing feature.
- ISUP recommends discontinuation of papillary RCCs into types 1 and 2, and instead recommends reporting specific **variants** with distinct morphology, immunoprofile, and clinical behavior whenever possible.

References:

1. Trpkov K, Hes O, Williamson SR, et al. New developments in existing WHO entities and evolving molecular concepts: The Genitourinary Pathology Society (GUPS) update on renal neoplasia. *Mod Pathol*. 2021 Jul;34(7):1392-1424.
2. Al-Obaidy KI, Eble JN, Cheng L, Williamson SR, Sakr WA, Gupta N, Idrees MT, Grignon DJ. Papillary Renal Neoplasm With Reverse Polarity: A Morphologic, Immunohistochemical, and Molecular Study. *Am J Surg Pathol*. 2019 Aug;43(8):1099-1111.
3. Kim SS, Cho YM, Kim GH, et al. Recurrent *KRAS* mutations identified in papillary renal neoplasm with reverse polarity—a comparative study with papillary renal cell carcinoma. *Mod Pathol*. 2020 Apr;33(4):690-699.
4. Deebajah M, et al. GATA3 Is a Useful Immunohistochemical Marker to Differentiate Variants of Renal Tubular Lesions from Different Segments of Renal Tubules, *American Journal of Clinical Pathology*, Volume 156, Issue Supplement_1, October 2021, Pages S152–S153
5. Van Esch H, Bilous RW. GATA3 and kidney development: why case reports are still important. *Nephrol Dial Transplant*. 2001 Nov;16(11):2130-2.
6. Cairns P. Renal cell carcinoma. *Cancer Biomark*. 2010;9(1-6):461-73.
7. Lindgren D, Sjölund J, Axelson H. Tracing Renal Cell Carcinomas back to the Nephron. *Trends Cancer*. 2018 Jul;4(7):472-484.





Case #6

Presenter: Hans Magne Hamnvåg, MD (PGY-III)

Attending: Dariusz Borys, MD

Clinical History: A 11-day old baby boy was brought to the clinic by his mother after she had noticed a mass on his right forearm while bathing him. There was no prior history of insect bites, trauma or falls, and the patient appeared comfortable and in no distress. The physical examination revealed a firm, subcutaneous, mobile, well-circumscribed mass on the forearm measuring 4.1 x 3.0 cm. The overlying skin was normal, with no surrounding erythema and no breaks in the skin. X-ray was performed which showed a large soft tissue mass involving the forearm. MRI demonstrated that the mass was homogenous in appearance and involved the muscular compartment of the forearm. The mass abutted the cortex of the mid radius, with a small amount of periosteal reaction present. An incisional biopsy was performed. A section from the biopsy is submitted for your review.

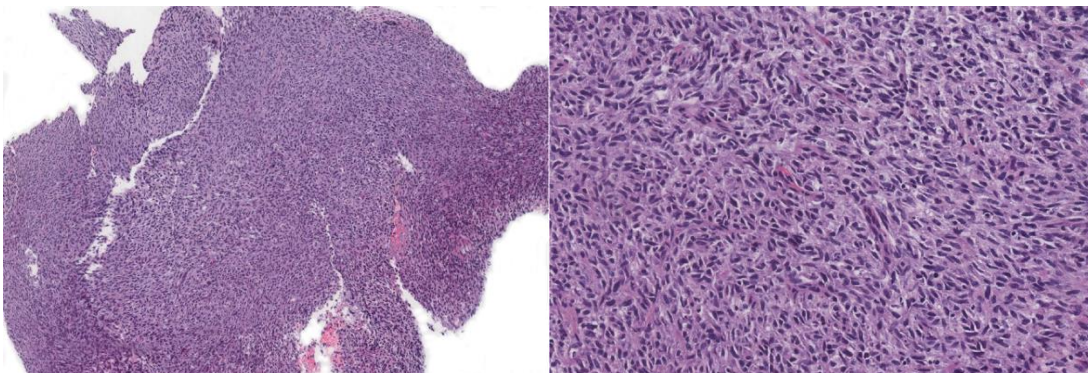
Final diagnosis: Infantile Fibrosarcoma

Differential Diagnosis:

- Spindle Cell Rhabdomyosarcoma
- Synovial Sarcoma
- Dermatofibrosarcoma Protruberans
- Solitary Fibrous Tumor

Key features:

Histopathology: Histological examination of the mass reveals spindle cells arranged in sheets and intersecting and sweeping fascicles. The tumor is uniformly cellular throughout the biopsy. The spindle cells are monomorphic, spindled to ovoid, and some cells have more angulated nuclei. Few mitoses were seen.





Positive IHC	Negative IHC
SMA (Focally)	Keratin AE1/AE3
	Desmin
	Myogenin
	Bcl-2
	CD34

Discussion:

Infantile Fibrosarcoma, also called Congenital Infantile Fibrosarcoma, is a rapidly growing infiltrative fibroblastic sarcoma. It is the second most common type of soft tissue sarcoma in infants and the most common occurring on the extremities. Around 75% of cases arise in the first year of life and is often congenital, with 40% of cases discovered at birth. The most common site of involvement is the superficial and deep soft tissues of the distal extremities, followed by trunk, and head and neck region. It is considered a locally aggressive tumor, with only rare cases of metastases reported. The tumor has a favorable prognosis in terms of mortality; however, the recurrence rate can be high, and the treatment can be associated with significant morbidity including amputation and debilitating surgeries.

The majority of Infantile Fibrosarcomas have a recurrent translocation t(12;15)(p13;q25) with translocation of genetic material between the *ETV6* gene on the short arm of chromosome 12 and the *NTRK3* gene located on the long arm of chromosome 15, resulting in a fusion gene involving the neurotrophic tyrosine receptor kinase-3 (*NTRK3*) gene, called *ETV6::NTRK3*. The *NTRK3* gene codes for Tropomyosin receptor kinase C, a tyrosine kinase that stimulates signaling proteins promoting growth, survival, and proliferation of cells. The tyrosine kinase of the *ETV6-NTRK3* fusion protein is continuously active, influencing numerous pathways that are known to be essential for proliferation, survival, angiogenesis, and invasion.

Surgical resection is still the pillar of treatment, however the surgical approach has evolved over the years from being the only treatment available, to being part of a multidisciplinary approach where initial neoadjuvant chemotherapy is used first to shrink the tumor prior to surgery, thus enabling the surgeon to spare more of the normal tissue. The latest drug that has been approved by the FDA for use in patients with Infantile Fibrosarcoma is Larotrectinib, which is a Tropomyosin receptor kinase inhibitor. Phase I trials have demonstrated that the drug is safe to use in both pediatric and adult patients, and individual case reports have started to emerge that reports successful use of Larotrectinib in locally aggressive inoperable Infantile Fibrosarcoma. Although the drug has been shown to result in tumor shrinkage in Phase I trials, larger trials comparing the efficacy of Larotrectinib versus standard of care on patient outcomes have still not been conducted.





Take Home Points:

- Infantile Fibrosarcoma is a locally aggressive soft tissue tumor, with often significant morbidity is associated with surgical resection
- New therapies targeting the *ETV6::NTRK3* gene fusion protein are emerging
- As a result of new emerging therapies, detection of the *ETV6::NTRK3* gene fusion will no longer only be used for diagnostic purposes, but also used to guide therapy

References:

1. Loh ML, Ahn P, Perez-Atayde AR, Gebhardt MC, Shamberger RC, Grier HE. Treatment of infantile fibrosarcoma with chemotherapy and surgery: results from the Dana-Farber Cancer Institute and Children's Hospital, Boston. *J Pediatr Hematol Oncol*. Dec 2002;24(9):722-6.
2. Sulkowski JP, Raval MV, Browne M. Margin status and multimodal therapy in infantile fibrosarcoma. *Pediatr Surg Int*. Aug 2013;29(8):771-6.
3. Chung EB, Enzinger FM. Infantile fibrosarcoma. *Cancer*. Aug 1976;38(2):729-39.
4. Coffin CM, Dehner LP. Soft tissue tumors in first year of life: a report of 190 cases. *Pediatr Pathol*. 1990;10(4):509-26.
5. Blocker S, Koenig J, Ternberg J. Congenital fibrosarcoma. *J Pediatr Surg*. Jul 1987;22(7):665-70.
6. Sandberg AA, Bridge JA. Updates on the cytogenetics and molecular genetics of bone and soft tissue tumors: congenital (infantile) fibrosarcoma and mesoblastic nephroma. *Cancer Genet Cytogenet*. Jan 1 2002;132(1):1-13.
7. Bourgeois JM, Knezevich SR, Mathers JA, Sorensen PH. Molecular detection of the ETV6-NTRK3 gene fusion differentiates congenital fibrosarcoma from other childhood spindle cell tumors. *Am J Surg Pathol*. Jul 2000;24(7):937-46.
8. Rubin BP, Chen CJ, Morgan TW, et al. Congenital mesoblastic nephroma t(12;15) is associated with ETV6-NTRK3 gene fusion: cytogenetic and molecular relationship to congenital (infantile) fibrosarcoma. *Am J Pathol*. Nov 1998;153(5):1451-8.
9. Orbach D, Brennan B, De Paoli A, et al. Conservative strategy in infantile fibrosarcoma is possible: The European paediatric Soft tissue sarcoma Study Group experience. *Eur J Cancer*. Apr 2016;57:1-9.
10. Chmielecki J, Bailey M, He J, et al. Genomic Profiling of a Large Set of Diverse Pediatric Cancers Identifies Known and Novel Mutations across Tumor Spectra. *Cancer Res*. Jan 15 2017;77(2):509-519. doi:10.1158/0008-5472.Can-16-1106.
11. Davis JL, Lockwood CM, Albert CM, Tsuchiya K, Hawkins DS, Rudzinski ER. Infantile NTRK-associated Mesenchymal Tumors. *Pediatr Dev Pathol*. Jan-Feb 2018;21(1):68-78.
12. DuBois SG, Laetsch TW, Federman N, et al. The use of neoadjuvant larotrectinib in the management of children with locally advanced TRK fusion sarcomas. *Cancer*. Nov 1 2018;124(21):4241-4247





13. Laetsch TW, DuBois SG, Mascarenhas L, et al. Larotrectinib for paediatric solid tumours harbouring NTRK gene fusions: phase 1 results from a multicentre, open-label, phase 1/2 study. *Lancet Oncol.* May 2018;19(5):705-714.
14. Jin W. Roles of TrkC Signaling in the Regulation of Tumorigenicity and Metastasis of Cancer. *Cancers (Basel).* Jan 8 2020;12
15. Slomovic A, Amaral T, Lobko I, et al. Comment on: A newborn with a large NTRK fusion positive infantile fibrosarcoma successfully treated with larotrectinib. *Pediatr Blood Cancer.* Jun 2021;68(6):e28953.

